SiRNA of Frizzled-9 suppresses proliferation and motility of hepatoma cells

TATSUYA FUJIMOTO, MINORU TOMIZAWA and OSAMU YOKOSUKA

Department of Medicine and Clinical Oncology, Graduate School of Medicine, Chiba University, 1-8-1 Inohana, Chuo-ku, Chiba City, Chiba 260-8670, Japan

Received May 12, 2009; Accepted July 9, 2009

DOI: 10.3892/ijo_00000400

Abstract. Frizzled (Fz), a receptor of Wnt ligands, plays key roles in liver carcinogenesis. Its expression was analyzed as part of a search for a target of molecular therapy for hepatocellular carcinoma (HCC) and hepatoblastoma (HB). Fz genes were analyzed by RT-PCR in HCC cell lines HLE, HLF, PLC/PRF/5, Huh-7 and Hep3B, HB cell lines Huh-6 and HepG2, HeLa cells, human normal fetal and adult liver. We transfected PLC/PRF/5, HLE, Huh-6, and HeLa cells with Fz9-small interfering RNA (Fz9-siRNA). Five days after transfection, cell proliferation was analyzed by MTS assay and cell motility by wound assay with H&E staining. Subsequently, the expressions of cyclin D1 and caspase-3 were analyzed by Western blot analysis. Fz9-siRNA decreased the expression of Fz9 gene in all cell lines. MTS assay showed that Fz9-siRNA significantly suppressed cell proliferation and cell motility in all cell lines. The expression of cyclin D1 was also suppressed by Western blotting. Cleaved caspase-3 did not appear and apoptosis was not observed in any of the cell lines tested. We demonstrated that Fz9 plays an essential role in carcinogenesis of HB and HCC, concluding that Fz9-siRNA could represent a useful therapeutic target for HB and HCC.

Introduction

The Wnt signalling pathway plays a crucial role in regulating cell growth and differentiation. Constitutive activation of the Wnt pathway causes abnormal cell growth and cancer (1-3). Frizzled (Fz) is a cell surface receptor that mediates the actions of Wnt ligands, and 10 members of the Fz family genes have been identified based on structural and functional homologies (4,5). Fz genes have been implicated in carcinogenesis and embryogenesis in previous studies. Their expressions are up-regulated in gastric, colon, breast, and renal cell carcinoma, suggesting that Fz genes are involved in carcinogenesis (6-12).

Regarding liver carcinogenesis, Fz genes play a crucial role. Hepatocellular carcinoma (HCC) arises in liver of Fz7 transgenic mice (13). Fz3, Fz6 and Fz7 genes are up-regulated in HCC tissues, compared with surrounding non-tumor tissues (14,15). However, because Fz3, Fz6 and Fz7 are expressed in surrounding non-tumor tissues, their clinically mediated inhibition may give rise to adverse effects. If a Fz gene would not be expressed in surrounding non-tumor tissues, it would be a good candidate for molecular therapy for HCC by inhibition of its activity. However, there is no literature on any Fz gene being expressed in tumor tissues while not expressed in surrounding non-tumor tissues. We thus analyzed the expressions of Fz genes of HCC cell lines, hepatoblastoma (HB) cell lines as well as HeLa cells, in an attempt to discover a novel therapeutic target.

Materials and methods

Cell lines and culture conditions. Human HB cell lines (Huh-6 and HepG2) and HCC cell lines (PLC/PRF/5, HLE, HLF, Huh-7 and Hep3B) were purchased from RIKEN Cell Bank (Tsukuba, Japan) and cultured in Dulbecco's minimum essential medium (DMEM; Sigma, St. Louis, MO) supplemented with 10% fetal bovine serum (FBS) (Trace Scientific, Melbourne, Australia) in 5% carbon dioxide at 37˚C in a humidified chamber. Cells were spread onto 10-cm dishes (Asahi Techno Glass, Funabashi, Japan) for Western blot analysis, 4-well chamber slides for wound assay (Iwaki, Tokyo, Japan), or 96-well flat bottom wells for proliferation assay (Asahi Techno Glass).

Reverse transcriptase-PCR. Total RNA (5 μg), isolated with Isogen (Nippon Gene, Tokyo, Japan), was used for first-strand cDNA synthesis with SuperScript III and oligo (dT) following the manufacturer's instructions (Invitrogen Japan K.K., Tokyo, Japan). RNAs of human fetal whole liver and human adult whole liver were purchased from Takara Bio (Kyoto, Japan). Polymerase chain reaction (PCR) was performed with Taq DNA polymerase (Applied Biosystems Japan, Tokyo, Japan). PCR primers, annealing temperature, number of cycles, and the length of the amplified products were as

Correspondence to: Dr Minoru Tomizawa, Department of Medicine and Clinical Oncology, Graduate School of Medicine, Chiba University, 1-8-1 Inohana, Chuo-ku, Chiba City, Chiba 260-8670, Japan
E-mail: nihminor-cib@umin.ac.jp

Key words: frizzled, siRNA, hepatocellular carcinoma, hepatoblastoma

below: Fz1 (GenBank accession no. NM_003505, 5'-AATG ACAAGTTCGCCGAGGAC, 5'-GCCAGGTGAAAATACT GTGAGTTGG; 59°C; 30 cycles, 206 bp), Fz2 (GenBank accession no. NM_001466, 5'-CAAGGTGCCATCCTAT CTCAGC, 5'-GTAGCAGCCCGACAGAAAAATG; 59°C; 30 cycles, 247 bp), Fz3 (GenBank accession no. NM_017412, 5'-AGAGAAGAACTGTCATTTGCTCGC, 5'-TCCTTGTG TCACTGTGGAAGCC; 53°C; 30 cycles, 255 bp), Fz4 (GenBank accession no. NM_012193, 5'-CAAGTGATTCTC CTGCCACAGC, 5'-CAACTCTCTCCAGTGTCCTCCATC; 57°C; 30 cycles, 270 bp), Fz5 (GenBank accession no. NM_003468, 5'-CCCTCATCCCCTAAGAGAGACAAAG, 5'-GCTGGCTGTGAAGAAGTTGCTG; 55°C; 30 cycles, 230 bp), Fz6 (GenBank accession no. NM_003506, 5'-AGC AGCATCCATCTCCAGACTCTC, 5'-CTGAATGACAACC ACCTCCCTG; 57°C; 30 cycles, 251 bp), Fz7 (GenBank accession no. NM_003507, 5'-AGACTTAGCCACAGCA GCAAGG, 5'-CGCCGTTATCATCATCTTCCTG; 58°C; 30 cycles, 287 bp), Fz8 (GenBank accession no. NM_031866, 5'-ATCCAAAGCAGATGCCATTGTC, 5'-AACACTGTGA AGGGGTGGGAAC; 59°C; 30 cycles, 137 bp), Fz9 (GenBank accession no. BC_026333, 5'-TCTTTGGAGAACCCCA CACACC, 5'-TGCTCACTTGCCTGACCTTGAC; 60°C; 30 cycles, 148 bp), Fz10 (GenBank accession no. NM_007197, 5'-AAACGCTGGACTGCCTGATG, 5'-GCTTTTTTGTAA ATCCCACCGC; 58°C; 30 cycles, 217 bp), GAPDH (GenBank accession no. NM_002046, 5'-ACCTGACCTGCCGTCTA GAA, 5'-TCCACCACCCTGTTGCTGTA; 63°C; 30 cycles, 246 bp).

SiRNA transfection. Transfection of siRNA of Fz9 (Fz9-siRNA) (Invitrogen Japan K.K.) was carried out using Lipofectamine 2000 (Invitrogen Japan K.K.) and Opti-MEN (Invitrogen Japan K.K.), according to the manufacturer's protocol. Briefly, siRNA and Lipofectamine 2000 were diluted in Opti-MEN at room temperature for 5 min, separately. Then the diluted siRNA and Lipofectamine 2000 were incubated for a further 20 min at room temperature for complex formation. The medium was aspirated from each dish or well, and the complexes were added to cultured cells. Transfection efficiency was analyzed as ~80% in PLC/PRF/5 and HeLa cell lines, and 90% in HuH-6 and HLE cell lines, respectively, with a fluorescein isothiocyanate (FITC)-labelled oligodeoxynucleotide (Invitrogen Japan K.K.) under this transfection condition (data not shown).

Cell viability assay. Freshly thawed cells were seeded onto 10-cm dishes. When they reached sub-confluence, they were trypsinized, harvested, and spread onto 96-well flat-bottom plates (Asahi Techno Glass) at a density of 1000 cells per well. Following 24 h of culture in DMEM with 10% fetal bovine serum, transfection was performed at a final concentration of 200 nM of siRNA in each well. As negative control, mock, Lipofectamine 2000 alone was used. Five days after transfection, 3-(4,5-dimethylthiazol-2-yl)-5-(3-carboxymethoxyphenyl)-2-(4-sulfophenyl)-2H-tetrazolium inner salt (MTS) assay was performed according to the manufacturer's instructions (Promega Corp., Tokyo, Japan). MTS is bioreduced by cells into a coloured formazan product that reduces absorbance at 490 nm. The absorbance was analyzed with a multiple plate reader at a wavelength of 490 nm with a Bio-Rad Model 550 microplate reader (Bio-Rad, Hercules, CA).

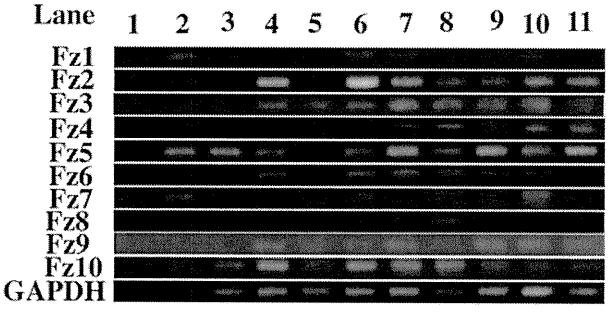

Figure 1. RT-PCR. Expression of human Fz genes was analyzed by RT-PCR with human fetal and adult liver, HCC and HB cell lines. A representative RT-PCR shows the expression of 10 Fz genes in H_2O (lane 1), human fetal whole liver (lane 2), human adult whole liver (lane 3), HeLa (lane 4), HLE (lane 5), HLF (lane 6), PLC/PRF/5 (lane 7), Huh-7 (lane 8), Hep3B (lane 9), Huh-6 (lane 10), HepG2 (lane 11). GAPDH was used as an endogenous control. Fz3 and Fz9 genes were expressed in HCC, HB, and HeLa (lanes 4-11), but not in normal fetal and adult liver (lanes 2 and 3).

Western blot analysis. Cells grown in culture dishes were transfected at ~70% confluence, at a final concentration of 200 nM of siRNA. At 5 days after transfection, the cells were harvested for Western blot analysis. Protein (20 μg) isolated from cultured cells was subjected to SDS-PAGE, and transferred to a nylon filter. The primary antibodies were polyclonal rabbit anti-human Fz9 (Lifespan Bioscience, Seattle, WA), polyclonal rabbit anti-human cyclin D1 (Cell Signalling Technology Japan K.K., Tokyo, Japan), monoclonal rabbit anti-human caspase-3 (Cell Signalling Technology Japan K.K.), and mouse monoclonal anti-α-tubulin antibody (Lab Vision, Fremont, CA). The second antibodies were HRP-linked anti-rabbit antibody (Amersham Bioscience, Tokyo, Japan) and HRP-linked anti-mouse antibody (Amersham Bioscience). Dilutions were 1:500 for the primary antibodies and 1:1000 for the second antibodies. The filters were reprobed with tubulin-α. The specific antigen-antibody complexes were visualized by enhanced chemiluminescence (Amersham Bioscience). The immunoreactive bands were normalized with tubulin-α and analyzed using Scion imaging software (Scion Imaging, Frederick, MD).

Wound assay. Cells were spread onto 4-well chambers (Iwaki). After 24 h, transfection was performed at a final concentration of 200 nM of siRNA in each well. Five days after transfection, sheets of cells were cut with a sterile razor. Two days later, cells were stained with hematoxylin-eosin and observed under a microscope. For each experiment, the number of cells migrating >50 μm of cut surface was counted in five different fields for each slide.

Statistical analysis. Cell proliferation was analyzed statistically with one-factor analysis of variance using Statview (version 5.0; SAS Institute Japan, Tokyo, Japan). A $P<0.05$ was accepted as statistically significant.

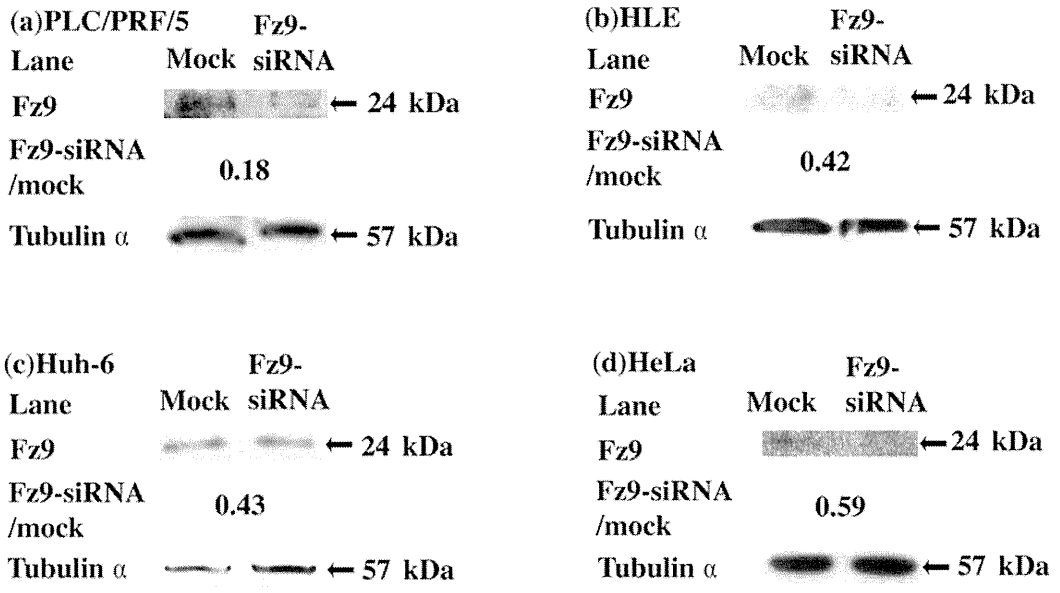

Figure 2. Western blot analysis of Fz9. The expression of Fz9 gene in PLC/PRF/5, HLE, Huh-6 and HeLa cells was examined by Western blotting with 20 μg of isolated protein 5 days after transfection of Fz9-siRNA. The expression of Fz9 gene was normalized against tubulin-α, a loading control, and the ratio of Fz9-siRNA to mock was calculated as Fz9-siRNA/Mock. Fz9 was down-regulated in cells transfected with Fz9-siRNA.

Results

Expression of Fz genes. The expressions of 10 Fz genes were analyzed by RT-PCR in human fetal and adult liver, and in HCC and HB cell lines. Fz3 and Fz9 genes were expressed in all HCC cell lines, HB cell lines and HeLa, but they were not expressed in normal fetal and adult liver (Fig. 1). Other Fz genes were expressed in normal fetal and adult liver.

Suppression of cell proliferation. First, we focused on Fz3, as it was expressed in HCC cell lines consistently according to a previous report (15). To investigate the role of Fz3 in cell proliferation, we transfected PLC/PRF/5, HLE, Huh-6 and HeLa cells with Fz3-siRNA. Five days after transfection, cell viability was analyzed by MTS assay. Fz3-siRNA did not suppress cell proliferation (data not shown). Fz9-siRNA was then transfected, and the expression of Fz9 was analyzed by Western blotting (Fig. 2). The expression level of Fz9 of cells transfected with Fz9-siRNA was observed to decrease compared to the corresponding mock in all cell lines (Fig. 2). MTS assay showed that Fz9-siRNA significantly suppressed the proliferation of all cell lines (Fig. 3).

Wound assay. Wound assay was performed to unveil the role of Fz9 in cell motility (Fig. 4). Fewer cells migrated >50 μm in PLC/PRF/5 cells than mock, while no cells migrated >50 μm in HLE, Huh-6 and HeLa cells, indicating that Fz9-siRNA significantly suppressed cell motility ($P<0.05$).

Western blot analysis. To determine the role of Fz9 in the cell cycle or apoptosis, the expressions of cyclin D1 and caspase-3 were analyzed by Western blotting (Fig. 5). The levels of cyclin D1 after Fz9-siRNA transfection decreased in all cell lines. On the other hand, the expression levels of

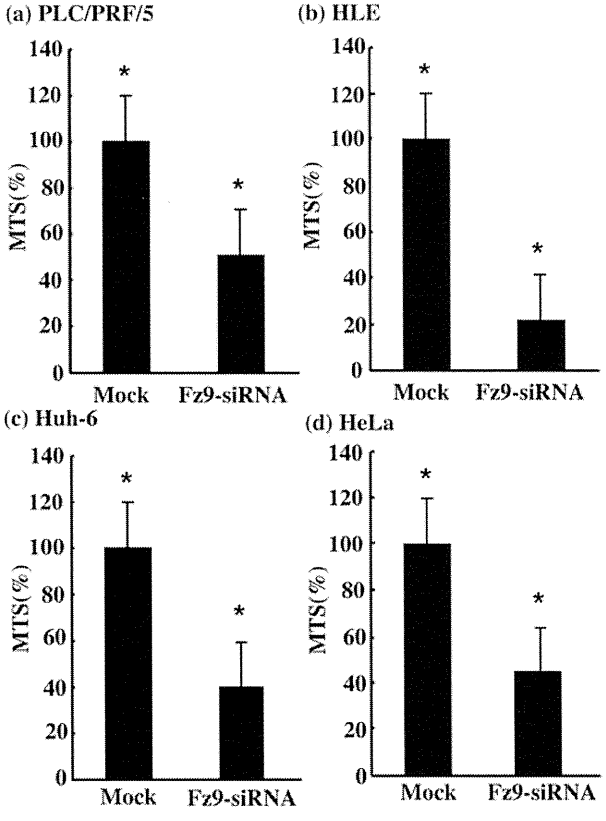

Figure 3. MTS assay. PLC/PRF/5, HLE, Huh-6, and HeLa, cells were transfected with Fz9-siRNA at a final concentration of 200 nM. Five days after transfection, cell viability was analyzed by MTS assay. Each value was normalized against the corresponding mock. Fz9-siRNA significantly suppressed the proliferation of all cell lines. *$P<0.05$.

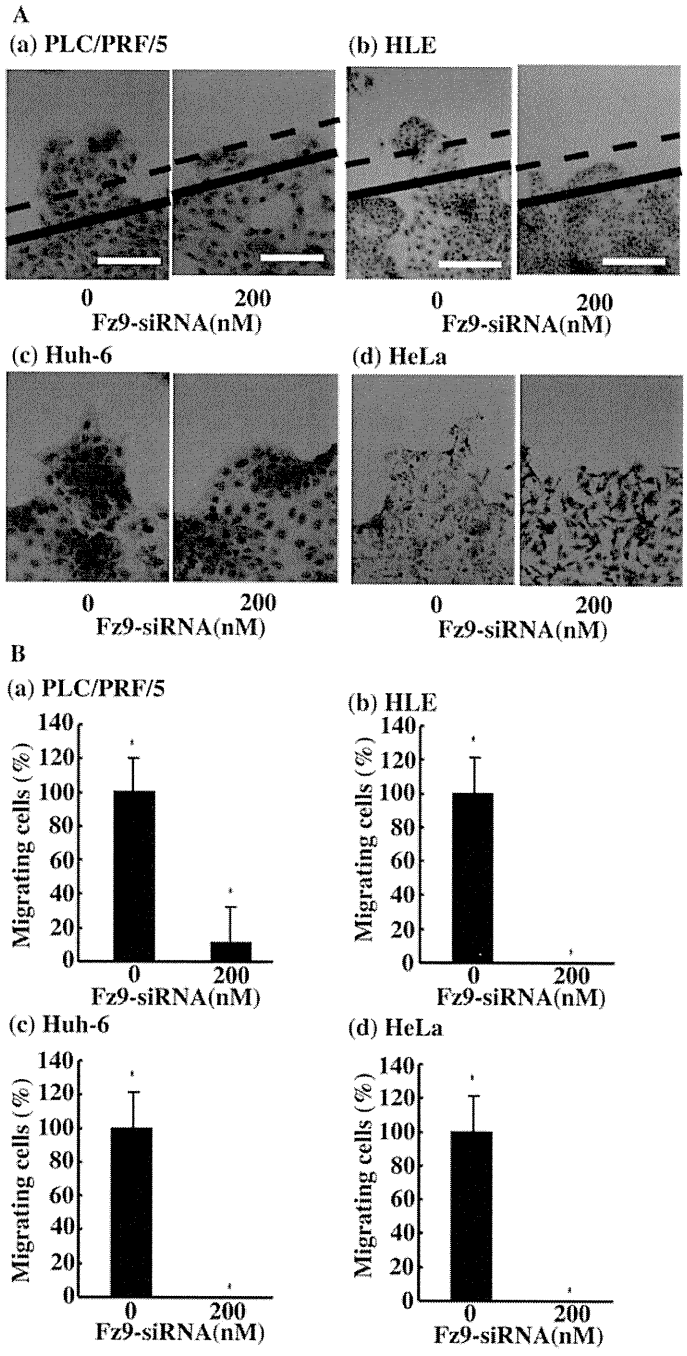

Figure 4. Wound assay. Wound assay was performed to analyze cell motility. Cells were transfected with Fz9-siRNA, stained with hematoxylin-eosin and observed under a microscope (A). The cells cultured with Fz9-siRNA and migrating >50 μm were counted, and normalized against the corresponding mock (migrating cell in B). Fz9-siRNA significantly suppressed cell motility in each cell line (B). (A) Original magnification x200; scale bar, 50 μm; (B) *P<0.05.

17 and 19 kDa of cleaved caspase-3, an essential element of apoptosis, did not appear. The expression levels of 35 kDa of caspase-3, a non-cleaved form, did not change. No pyknotic cells were found in any of the cell lines transfected with Fz9-siRNA (Fig. 4A).

Discussion

Human Fz9 is expressed in the brain, testis, eye, skeletal muscle and kidney, but not in liver (16). Our RT-PCR also showed no expression of Fz9 gene in human adult liver, consistent with the previous report. This finding suggested that Fz9 played only a slight role in liver development. Since Fz9 is expressed in brain and skeletal muscle, its deletion causes musculoskeletal anomalies and neurological problems in Williams syndrome (16,17). Fz9 expression in human astocytoma and glioblastoma was significantly higher than in normal brain (18). Interestingly, Fz9 is not originally expressed in astrocytes, and tumor cells acquired the expression of Fz9 (19). The expression level of Fz9 increases as tumor cells

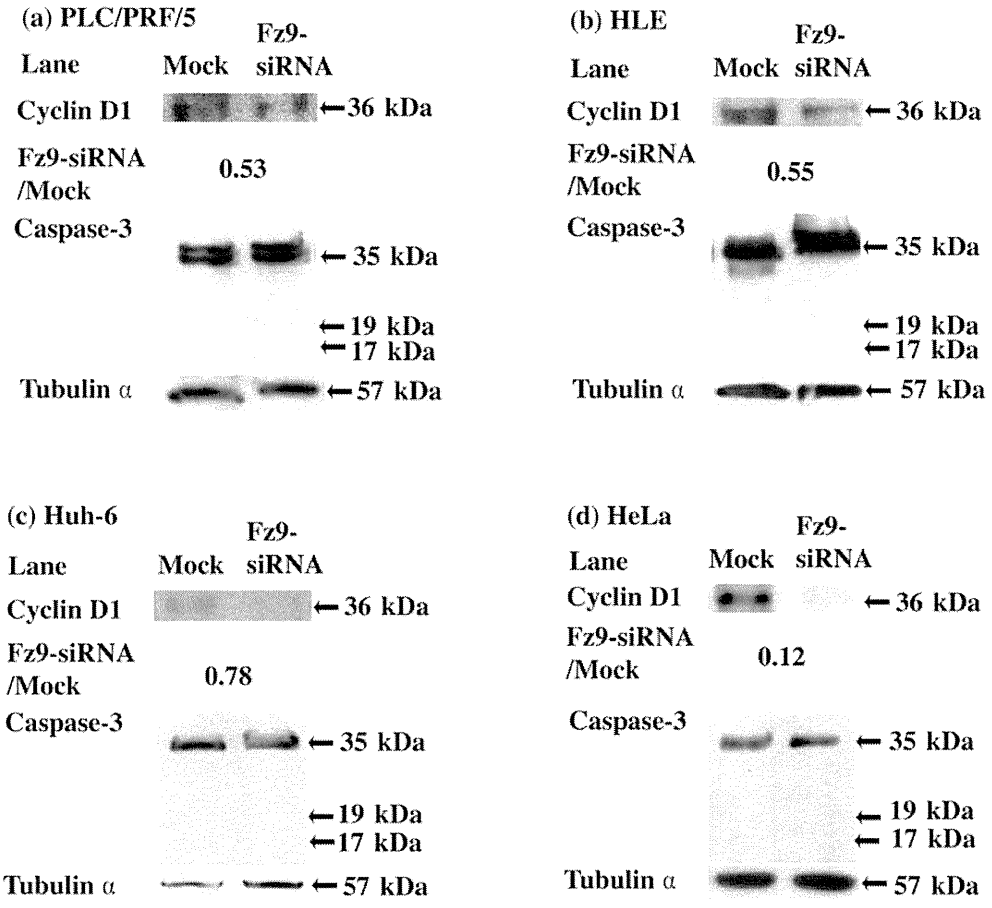

Figure 5. Western blot analysis of cyclin D1 and caspase-3. Effect of Fz9-siRNA on cell cycle and apoptosis. Western blot analysis was performed with cyclin D1 and caspase-3 in PLC/PRF/5, Huh-6, HeLa, and HLE cells transfected with Fz9-siRNA. Tubulin-α served as a loading control. Fz9-siRNA/mock, a ratio of the cyclin D1 expression level normalized against tubulin-α in cells transfected with Fz9-siRNA divided by that in mock. Fz9-siRNA suppressed the expression of cyclin D1. The expression levels of 17 and 19 kDa of cleaved caspase-3, an essential element for apoptosis, were not detected in any of the cells.

become less differentiated. Increased expression of Fz9 is involved in the carcinogenesis of astrocytoma and glioblastoma, and the expression of Fz9 increased markedly in colorectal cancer compared to normal tissues (10). Our results showed that Fz9 was expressed in all cell lines, and indicated that Fz9 was involved in carcinogenesis, although the detailed mechanisms remained elusive. The biological significance of the result that Fz9 was expressed in HCC and HB cell lines still needs to be unravelled. MTS assay revealed that Fz9-siRNA significantly suppressed the proliferation of all cell lines. We then used Western blotting to examine the expression of cyclin D1, known to be deeply involved in the cell cycle (Fig. 5), and found it to be significantly down-regulated in all cell lines transfected with Fz9-siRNA. Subsequently, caspase-3, a target effecter of apoptosis, was analyzed. Its cleaved form was not detected at all, while the expression level of the 35 kDa form was not changed. This indicates that Fz9 suppressed cell proliferation via the cell cycle, not through apoptosis. This hypothesis was supported by the result of H&E staining, that pyknotic cells were not observed (Fig. 4A).

A previous study reported that Fz3, Fz6 and Fz7 were up-regulated in tumor tissues compared to non-tumor ones (15). In our experiments, Fz6 and Fz7 were not expressed in any of the cell lines tested, while Fz3 and Fz9 were expressed in all cell lines. These discrepancies could be explained by the fact that our study did not use quantitative RT-PCR, possibly obscuring differences in expression levels. Fz3 was a good candidate for molecular therapy since it was expressed in all cell lines and not in fetal and adult liver in our study, and it was up-regulated in tumor tissues in the previous study. Fz3-siRNA failed to suppress cell proliferation. The reason is not known, but Fz3 might not be involved in cell proliferation in HCC and HB.

Our result was the first concerning Fz9 being expressed in HCC and HB cell lines and not in fetal and adult liver. The previous report did not show its up-regulation. The reason for this discrepancy might be that tumor tissues contained non-cancer cells, such as blood and endothelial cells, and the expression level of Fz9 might have been obscured. Our study was more accurate with pure cancer cell lines.

Fz7-siRNA suppressed cell proliferation (9). However, as it was expressed in fetal and adult liver in our results, it was not suitable for molecular therapy. On the other hand, because of its non-expression in fetal and adult liver, Fz9 was considered potentially useful. No adverse effects were

anticipated if Fz9-siRNA were applied in a clinical situation, since Fz9-siRNA would not be expected to affect surrounding normal liver. Fz9-siRNA may thus prove to be useful in a clinical setting.

In conclusion, we demonstrated that Fz9 played an essential role in cell proliferation and motility of HB and HCC. It was considered possible that Fz9 gene could represent a promising target for novel molecular therapy in HCC as well as HB.

Acknowledgements

This research was supported by a Research Grant-in-Aid for Scientific Research (C) from the Japan Society for the Promotion of Science (19590748).

References

1. Katoh M: WNT signaling pathway and stem cell signaling network. Clin Cancer Res 13: 4042-4045, 2007.
2. Katoh M: WNT signaling in stem cell biology and regenerative medicine. Curr Drug Targets 9: 565-570, 2008.
3. Nusse R: Wnt signaling and stem cell control. Cell Res 18: 523-527, 2008.
4. Bhanot P, Brink M, Samos CH, *et al*: A new member of the frizzled family from Drosophila functions as a Wingless receptor. Nature 382: 225-230, 1996.
5. Wang HY, Liu T and Malbon CC: Structure-function analysis of Frizzleds. Cell Signal 18: 934-941, 2006.
6. Kirikoshi H, Sekihara H and Katoh M: Expression profiles of 10 members of Frizzled gene family in human gastric cancer. Int J Oncol 19: 767-771, 2001.
7. Vincan E, Darcy PK, Smyth MJ, *et al*: Frizzled-7 receptor ectodomain expression in a colon cancer cell line induces morphological change and attenuates tumor growth. Differentiation 73: 142-153, 2005.
8. Vincan E, Darcy PK, Farrelly CA, Faux MC, Brabletz T and Ramsay RG: Frizzled-7 dictates three-dimensional organization of colorectal cancer cell carcinoids. Oncogene 26: 2340-2352, 2007.
9 Ueno K, Hiura M, Suehiro Y, *et al*: Frizzled-7 as a potential therapeutic target in colorectal cancer. Neoplasia 10: 697-705, 2008.
10. Nagayama S, Yamada E, Kohno Y, *et al*: Inverse correlation of the up-regulation of FZD10 expression and the activation of beta-catenin in synchronous colorectal tumors. Cancer Sci 100: 405-412, 2009.
11. Milovanovic T, Planutis K, Nguyen A, *et al*: Expression of Wnt genes and frizzled 1 and 2 receptors in normal breast epithelium and infiltrating breast carcinoma. Int J Oncol 25: 1337-1342, 2004.
12. Janssens N, Andries L, Janicot M, Perera T and Bakker A: Alteration of frizzled expression in renal cell carcinoma. Tumour Biol 25: 161-171, 2004.
13. Merle P, Monte S, Kim M, *et al*: Functional consequences of frizzled-7 receptor overexpression in human hepatocellular carcinoma, Gastroenterology 127: 1110-1122, 2004.
14. Merle P, Kim M, Herrmann M, *et al*: Oncogenic role of the frizzled-7/beta-catenin pathway in hepatocellular carcinoma. J Hepatol 43: 854-862, 2005.
15. Bengochea A, Souza MM, Lefrancois L, *et al*: Common dysregulation of Wnt/Frizzled receptor elements in human hepatocellular carcinoma. Br J Cancer 99: 143-150, 2008.
16. Wang YK, Samos CH, Peoples R, Perez-Jurado LA, Nusse R and Francke U: A novel human homologue of the Drosophila frizzled wnt receptor gene binds wingless protein and is in the Williams syndrome deletion at 7q11.23. Hum Mol Genet 6: 465-472, 1997.
17. Wang YK, Sporle R, Paperna T, Schughart K and Francke U: Characterization and expression pattern of the frizzled gene Fzd9, the mouse homolog of FZD9 which is deleted in Williams-Beuren syndrome. Genomics 57: 235-248, 1999.
18. Zhang Z, Schittenhelm J, Guo K, *et al*: Upregulation of frizzled 9 in astrocytomas. Neuropathol Appl Neurobiol 32: 615-624, 2006.
19. Rawal N, Castelo-Branco G, Sousa KM, *et al*: Dynamic temporal and cell type-specific expression of Wnt signaling components in the developing midbrain. Exp Cell Res 312: 1626-1636, 2006.

Scandinavian Journal of Gastroenterology, 2009; 44: 872–877

informa
healthcare

ORIGINAL ARTICLE

Quantification of hepatitis C amino acid substitutions 70 and 91 in the core coding region by real-time amplification refractory mutation system reverse transcription-polymerase chain reaction

SHINGO NAKAMOTO, TATSUO KANDA, YUTAKA YONEMITSU, MAKOTO ARAI, KEIICHI FUJIWARA, KENICHI FUKAI, FUMIHIKO KANAI, FUMIO IMAZEKI & OSAMU YOKOSUKA

Department of Medicine and Clinical Oncology, Graduate School of Medicine, Chiba University, Chiba, Japan

Abstract

Objective. The effects of hepatitis C virus (HCV) sequence variations on the success of antiviral therapy or the development of hepatocellular carcinoma (HCC) are complex for many reasons. Recently, there have been several reports on the effects of genotype 1b HCV core amino acid substitutions 70 and/or 91 on the outcome of antiviral therapies and the clinical course. The purpose of this study was to establish real-time amplification refractory mutation system (ARMS) reverse transcription (RT)-polymerase chain reaction (PCR) assays for easy detection of these HCV mutations. ***Material and methods.*** Plasmids p-core-W, including the wild-type HCV core coding region (70R and 91L), and p-core-M, including the mutant-type HCV core (70Q and 91M), were constructed by cloning and PCR-based mutagenesis for control vector of the wild-type core and that of the mutant core, respectively. Using serially diluted forms of these vectors, SyBr Green-based real-time ARMS RT-PCR detection with each of the specific primer pairs was performed. ***Results.*** Each primer could clearly distinguish the difference between p-core-W and p-core-M at the same copy numbers. Concerning substitution 70, the ratios 100:1, 10:1, 1:1, 1:10, and 1:100 of p-core-W versus p-core-M could be distinguished, while for substitution 91, the ratios 100:1, 10:1, 1:1, 1:10, 1:100, and 1:1000 could be distinguished, confirming the sensitivity and specificity of the assay. ***Conclusions.*** This method could be a useful alternative for the detection of genotype 1b HCV core amino acid substitutions 70 and 91 and be reliably applied for rapid screening.

Key Words: *ARMS, core, HCV, interferon response, real-time PCR*

Introduction

More than 170 million people world-wide are chronically infected with hepatitis C virus (HCV), which can lead to hepatic cirrhosis and hepatocellular carcinoma (HCC) [1]. Treatment with peginterferon and ribavirin for 24–48 weeks can result in a sustained loss of serum HCV-RNA (termed a sustained virological response (SVR)), with resolution of chronic hepatitis in approximately half of the patients [2]. Several new, potent HCV protease and polymerase inhibitors have been described recently, but none of them are available for therapeutic use.

The genomic region encoding the HCV core protein is located between amino acids 1 and 191 and is likely to be the first gene product synthesized due to its localization at the 5′ end of the HCV polyprotein transcript [3]. The core protein has an ability to interact with the viral genomic region to form nucleocapsids [4], and the presence of a putative DNA-binding motif, nuclear localization signals, phosphorylation sites, and a nucleocytoplasmic localization of the core protein suggest its possible function as a gene regulatory protein [3,5]. In many previous studies it has been suggested that the HCV core protein may be important in hepatocarcinogenesis and interferon signaling [3,6–8].

HCV genotype 1b is a major genotype (~70%) in Japan. HCV genotype 1 is one of the most refractory to interferon treatment with or without ribavirin. It has been reported that its response to interferon

Correspondence: Tatsuo Kanda, MD, PhD, Department of Medicine and Clinical Oncology, Graduate School of Medicine, Chiba University, 1-8-1 Inohana, Chuo-ku, Chiba 260-8677, Japan. Tel: +81 43 2262 086. Fax: +81 43 2262 088. E-mail: kandat-cib@umin.ac.jp

(Received 5 February 2009; accepted 29 March 2009)

ISSN 0036-5521 print/ISSN 1502-7708 online
DOI: 10.1080/00365520902937362

monotherapy is affected by HCV NS5A gene diversity [9]. Thus, sequence diversity may predict the response to the combination therapy of peginterferon and ribavirin. Furthermore, ribavirin has different antiviral effects from those of interferon [10]. An approach to the prediction of treatment against hepatitis C in patients who do not have SVR is urgently needed. Several reports suggest that HCV amino acid substitutions 70 and 91 in the core coding region affect the results of combination therapies of interferon and ribavirin [11–13], but most of these studies were retrospective, and we do not know whether these substitutions already existed before treatment or were selected by the treatment. A sensitive, real-time polymerase chain reaction (PCR)-based assay for the detection of these mutations in the presence of high levels of wild-type virus is described here. The method is based on the amplification refractory mutation system (ARMS) reverse transcription (RT)-PCR for detection of single base mutations [14,15].

Material and methods

Plasmid DNA controls

Plasmids carrying HCV genotype 1 b core wild-type and mutant clones were made as described previously [16,17] and are summarized in Table I. Plasmid DNA was purified using the QIAprep spin miniprep kit (Qiagen, Hilden, Germany). Plasmids were serially diluted 1:10 in EASY dilution (for real-time PCR) (Takara, Ohtsu, Shiga, Japan) to give a dilution range of $1–1 \times 10^9$ copies for controls of real-time PCR.

Extraction of HCV-RNA from serum

Serum samples (100 µl) were extracted using the high pure viral RNA kit (Roche Diagnostics, Indianapolis, Ind., USA) according to the manufacturer's protocol. The RNA was eluted in RNase-free water. Written informed consent was obtained from each patient included in this study.

cDNA synthesis and SyBr Green real-time PCR

Reverse transcription was carried out using random hexamers to make HCV cDNA by superscript cDNA synthesis kit (Invitrogen, Carlsbad, Calif., USA). ARMS primers were designed so that the 3′ base matched either the wild-type or mutant sequence [18] (Table II). Each 25-µl reaction contained 2× Power SYBR Green PCR Master Mix (Applied Biosystems, Tokyo, Japan), 2.5 pmol of each primer (Table II). Reactions were run on the Step One real-time PCR system (Applied Biosystems). Cycling conditions were: denaturation at 95°C for 10 min, then 40 cycles at 95°C for 15 s and 60°C for 1 min, followed by a melting curve analysis, confirming their specificity. A plasmid DNA standard was included in each run.

Cloning of clinical HCV sequences and site-directed mutagenesis

To make the plasmid p-core-mutant, PCR products were cloned into pCR-TOPO2.1 vector (Invitrogen). To make the plasmid p-core-wild, PCR-based *in vitro* site-directed mutagenesis was performed using the Quick Change site-directed mutagenesis kit (Stratagene, La Jolla, Calif., USA). DNA sequences of clones were confirmed by direct sequencing.

Results

Optimization of real-time PCR

For this study, real-time PCR using the SYBR Green I detection system (Applied Biosystems) was implemented to detect the HCV amplicon. ARMS PCR specificity is conferred by direct placement of the 3′ end of one of the primers (Figure 1). Cross-reactivity was tested to ensure that the primer sets specifically bound their targets.

When 10^8 copies of the CAA (codon c70) template were amplified using the primer with a base mismatch, approximately 15 cycles were required before the crossing threshold was reached. This compares with 8 cycles for the matching primer. On the other hand, when 10^8 copies of the CGA (codon c70) template were amplified using the primer with a base mismatch, approximately 16 cycles were required before the crossing threshold was reached. This compares with 6 cycles for the matching primer (Figure 1A and B).

When 10^8 copies of the ATG (codon c91) template were amplified using the primer with a base mismatch, approximately 25 cycles were required before the crossing threshold was reached. This compares

Table I. Plasmid DNA used as standard in this study.

Plasmid	Amino acid c70	Codon c70	Amino acid c91	Codon c91
p-core-wild	Arginine	CGA	Leucine	CTG
p-core-mutant	Glutamine	CAA	Methionine	ATG

Table II. Primers used for detection of substitutions at residues c70 (A) and c91 (B).

A.

Primers for detection of substitution at c70		
Primer common to all reactions		
c70 sense primers HCV-c-reverse: 5′-CGGGGTGACAGGAGCCATCC-3′	Codon	Amino acids
HCV 70W: 5′-TATCCCCAAGGCTCGCCG-3′	CGN	Arg
HCV 71M: 5′-TATCCCCAAGGCTCGCCA-3′	CAN	Gln, His

N = A, G, T, or C; Arg = arginine; Gln = glutamine; His = histidine.

B.

Primers for detection of substitution at c91		
Primer common to all reactions		
c91 reverse primers HCV-c-sense: 5′-TCGCAACCTCGTGGAAGGC-3′	Codon	Amino acids
HCV 91W: 5′-CATCCTGCCCACCCCAR-3′	TTG or CTG	Leu
HCV 91M: 5′-CATCCTGCCCACCCCAT-3′	ATG	Met

R = A, G; Met = methionine; Leu = leucine.
HCV sequences are identical to AJ238799. Ref. [11].

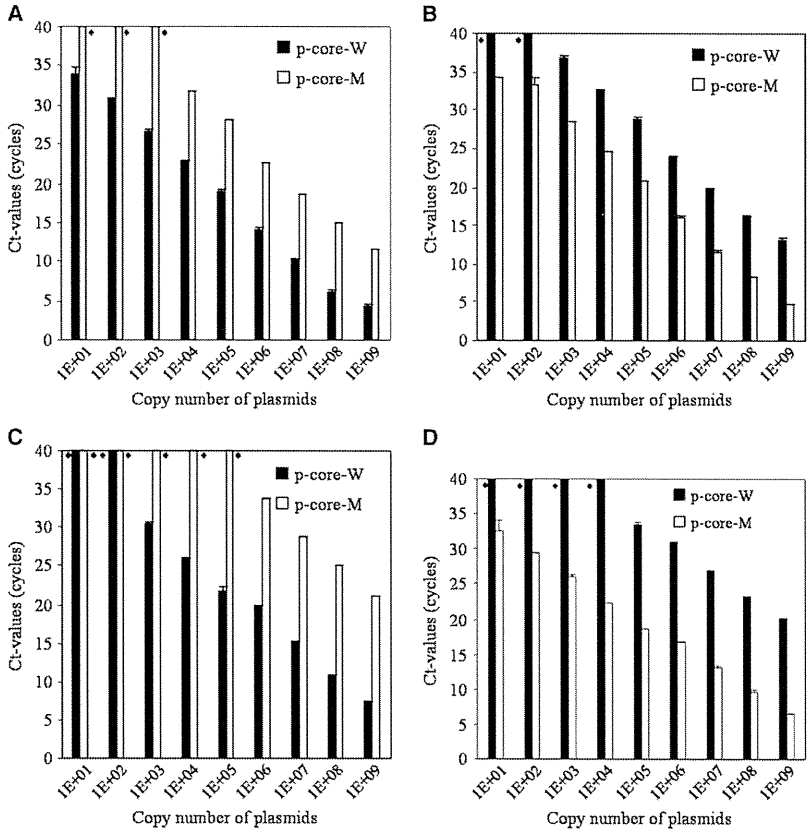

Figure 1. Quantitation of a 10-fold dilution of plasmid p-core-W or p-core-M with wild- or mutant-type primers. Cycle numbers were plotted against the logarithmic concentration of serial dilutions. A. c70-wild primer sets (HCV-70W and HCV-c-reverse). B. c70-mutant primer sets (HCV-70M and HCV-c-reverse). C. c91-wild primer sets (HCV-c-sense and HCV-91W). D. c91-mutant primer sets (HCV-c-sense and HCV-91M). *Unable to detect any signals by 40 cycles.

with 10 cycles for the matching primer. On the other hand, when 10^8 copies of the CTG (codon c91) template were amplified using the primer with a base mismatch, approximately 23 cycles were required before the crossing threshold was reached. This compares with 10 cycles for the matching primer (Figure 1C and D).

The detection limits of these methods were at least 10 copies, 10 copies, 1000 copies, and 10 copies of c70-wild primer sets (HCV-70W and HCV-c-reverse), c70-mutant primer sets (HCV-70M and HCV-c-reverse), c91-wild primer sets (HCV-c-sense and HCV-91W), and c91-mutant primer sets (HCV-c-sense and HCV-91M), respectively (Figure 1).

Selectivity of ARMS assay

Using the plasmid mixture containing the wild-type (p-core-W) and the mutant-type (p-core-M) as a template, real-time ARMS PCR was performed to establish the concentration at which the c70-wild primer sets (HCV-70W and HCV-c-reverse) would detect the wild-type DNA (codon c70). In Table IIIA we present the results of these primer sets showing that, when the wild DNA was 10^9 copies/tube, from 10^5 to 10^9 copies of mutant templates did not affect the results. When the mutant DNA was 10^9 copies/tube, from 10^9 to 10^7 copies of the wild templates could be detected. Similarly, each primer could clearly distinguish the difference between p-core-W and p-core-M at the same copy numbers. Concerning substitution 70, the ratios 100:1, 10:1, 1:1, 1:10, and 1:100 of p-core-W versus p-core-M could be distinguished (Table IIIA and B). However, for substitution 91, the ratios 100:1, 10:1, 1:1, 1:10, 1:100, and 1:1000 could be distinguished, confirming the sensitivity and specificity of the assay [16] (Table IIIC and D).

Hepatitis C core substitutions in serum by real-time ARMS RT-PCR

Quantitative ARMS assays were carried out in parallel reactions, one with a primer matching the variant at the 3′ end, and the other with the primer matching the wild-type variant. We measured the HCV core substitutions at residues c70 and c91 in two patients who did not respond to combination peginterferon and ribavirin therapy after 12 weeks and finally did not become SVRs (Table IV). In patient no. 1, we could detect the minority, wild-type at c70 (4% at 4 weeks). This became diminished at 12 weeks after treatment. In both patients, we could not detect any wild-type template at 12 weeks after treatment.

Comparison of real-time ARMS RT-PCR and conventional sequencing

The real-time ARMS RT-PCR method was compared to direct sequencing in patients treated with peginterferon and ribavirin. In patient no. 1, the minority, wild-type at c70 at 4 weeks could not be detected by direct sequencing (Table IV). In patient no. 2, there were some discrepancies between the results of direct sequencing and those of real-time ARMS RT-PCR (Table IV).

Table III. A mixture of the dilution series of mutants with fixed concentration of wild-type DNA or mutant-type DNA was assayed with each primer to establish the concentration at which the primers would detect each DNA by real-time ARMS PCR. Copy number: copies/tube; template W: p-core-W; template M: p-core-M.

Copy number of template (W:M)	Ct (cycle number)
A. c70-wild primer sets (HCV-70W and HCV-c-reverse).	
10^5:10^9	12.66±0.050
10^6:10^9	12.47±0.099
10^7:10^9	11.46±0.036
10^8:10^9	8.87±0.279
10^9:10^9	5.29±0.018
10^9:10^8	5.24±0.075
10^9:10^7	5.24±0.070
10^9:10^6	5.15±0.091
10^9:10^5	5.13±0.014
B. c70-mutant primer sets (HCV-70M and HCV-c-reverse).	
10^9:10^5	14.44±0.026
10^9:10^6	14.18±0.017
10^9:10^7	12.66±0.044
10^9:10^8	9.68±0.041
10^9:10^9	6.00±0.126
10^8:10^9	5.72±0.10
10^7:10^9	5.57±0.028
10^6:10^9	5.90±0.072
10^5:10^9	5.77±0.063
C. c91-wild primer sets (HCV-c-sense and HCV-91W).	
10^5:10^9	22.77±0.197
10^6:10^9	20.99±0.182
10^7:10^9	17.46±0.0457
10^8:10^9	13.36±0.10
10^9:10^9	9.30±0.053
10^9:10^8	9.29±0.12
10^9:10^7	9.19±0.043
10^9:10^6	9.14±0.060
10^9:10^5	9.23±0.0011
D. c91-mutant primer sets (HCV-c-sense and HCV-91M).	
10^9:10^5	20.89±0.056
10^9:10^6	18.52±0.351
10^9:10^7	14.89±0.016
10^9:10^8	11.53±0.033
10^9:10^9	7.99±0.023
10^8:10^9	7.82±0.0040
10^7:10^9	7.80±0.0098
10^6:10^9	7.86±0.044
10^5:10^9	7.82±0.0025

Table IV. HCV core substitutions at residues c70 and c91 detected by real-time ARMS RT-PCR and direct sequencing.

Patients No.	Study Week	ALT (IU/L)	HCV-RNA (log copies/ml)	c70 W:M	c91 W:M	Direct sequencing c-70/c-91
1.	0	31	6.6	0:100	0:100	M/M
	4	26	6.3	4:96	0:100	M/M
	12	24	5.8	0:100	0:100	M/M
2.	0	53	6.3	0:100	ND	Mix/M
	4	25	6.0	0:100	0:100	M/M
	12	14	5.3	0:100	0:100	M/M

Abbreviations: ARMS = amplification refractory mutation system; ALT = alanine aminotransferase; W = wild-type; M = mutant-type; Mix = mixed-type; ND = not determined.
"Study Week" = weeks after administration of peginterferon and ribavirin.

Discussion

In this article we describe a rapid and sensitive method for the quantitative detection and monitoring of the core amino acid substitutions of HCV genotype 1b. SyBr Green real-time PCR and specific ARMS primers were used to quantify viral RNAs carrying particular sequences, HCV amino acid substitutions 70 and 91 in the core coding region. The specificity of the ARMS primers results in large differences in PCR crossing thresholds being observed between matching and mismatched targets.

For the current standard treatment with peginterferon alpha and ribavirin in patients with chronic hepatitis C, infection with HCV genotypes 2 and 3, lower baseline viral load, Asian and Caucasian ethnicity, younger age, low γ-GTP levels, absence of advanced fibrosis/cirrhosis, and absence of steatosis in the liver have been identified as independent pretreatment predictors of SVR [19]. Early virological response (EVR), defined as a $\geq$2-log reduction in HCV-RNA or undetectable HCV-RNA at 12 weeks, is associated with a favorable virological response. EVR is reached in only ~70% of patients infected with genotype 1 treated with combination therapy [20,21].

Recently, it was reported that core residues Arg70 and Leu91 were associated with response therapy in Japanese genotype 1b patients [11,13]. Donlin et al. [12] reported a similar association of Arg70 with a marked response for genotype 1b but not 1a; however, Met91 was highly dominant in both the marked- and poor-responder sequences, but few other studies have examined the role of diversity in the core in the outcome of therapy. Concerning hepatocarcinogenesis associated with HCV genotype 1b, Akuta et al. [22] reported that cumulative hepatocarcinogenesis rates in double wild-type (Arg70 and Leu91) of the HCV core region were significantly lower than those in non-double wild-type. Direct sequencing [11,13] and nested-RT-PCR using ARMS primers with gel electrophoresis [12,22] were performed in these studies. Higher sensitivity assays may be more useful for predicting the outcomes of therapy and hepatocarcinogenesis [23]. The real-time ARMS RT-PCR described here does not require restriction enzyme digestion, gel-electrophoresis or sequence analysis of PCR products, and it can quantify the core substitution proportions more quickly.

Hepatitis C core substitutions in serum detected by real-time ARMS RT-PCR showed mutant c70 and mutant c91 at 12 weeks in two non-EVRs (Table IV). Most non-SVR rates result from non-EVR. It was reported that the 72-week regimen significantly improved the SVR rates in non-EVRs with Arg70 and/or Leu91 of core [24]. Peginterferon plus ribavirin treatment is costly and has several side effects, possibly reducing its attractiveness for patients. If we were able to identify these HCV core substitutions at 12 weeks, we would know whether to stop or continue treating patients. This could prevent patients from serious side effects or bring about a better treatment outcome by the resulting shorter regimens. Moreover, if direct viral enzyme inhibitors such as protease inhibitor and polymerase inhibitor, which potently suppress viral replication, could be used, the predictability of outcome would be even more important. Recently, it was also reported that maintenance or prolonged peginterferon did not reduce the incidence of HCC in advanced chronic hepatitis C patients [1,25]. We are now focusing on a larger study, and real-time ARMS RT-PCR is expected to be useful for the important prediction of peginterferon plus ribavirin treatment outcomes or that of hepatocarcinogenesis in hepatitis C patients.

Acknowledgements

We thank Professor M. Omata, Department of Gastroenterology, University of Tokyo, for invaluable discussions. This work was supported by the Ministry of Education, Culture, Sports, Science and Technology, Japan (TK, OY).

Declaration of interest: The authors report no conflicts of interest. The authors alone are responsible for the content and writing of the paper.

References

[1] Di Bisceglie AM, Shiffman ML, Everson GT, Lindsay KL, Everhart JE, Wright EC, et al. Prolonged therapy of advanced chronic hepatitis C with low-dose peginterferon. N Engl J Med 2008;359:2429–41.

[2] George SL, Bacon BR, Brunt EM, Mihindukulasuriya KL, Hoffmann J, Di Bisceglie AM. Clinical, virologic, histologic, and biochemical outcomes after successful HCV therapy: a 5-year follow-up of 150 patients. Hepatology 2008; Epub ahead of print.

[3] Basu A, Meyer K, Ray RB, Ray R. Hepatitis C virus core protein modulates the interferon-induced transacting factors of Jak/Stat signaling pathway but does not affect the activation of downstream IRF-1 or 561 gene. Virology 2001;288:379–90.

[4] Shimoike T, Mimori S, Tani H, Matsuura Y, Miyamura T. Interaction of hepatitis C virus core protein with viral sense RNA and suppression of its translation. J Virol 1999;73: 9718–25.

[5] Otsuka M, Kato N, Lan K-H, Yoshida H, Kato J, Goto T , et al. Hepatitis C core protein enhances p53 function through augmentation of DNA binding affinity and transcriptional ability. J Biol Chem 2000;275:34122–30.

[6] Kanda T, Steele R, Ray R, Ray RB. Hepatitis C virus core protein augments androgen receptor-mediated signaling. J Virol 2008;82:11066–72.

[7] Pavio N, Battaglia S, Boucreux D, Arnulf B, Sobesky R, Hermine O, et al. Hepatitis C virus core variants isolated from liver tumor but not from adjacent non-tumor tissue interact with Smad3 and inhibit the TGF-beta pathway. Oncogene 2005;24:6119–32.

[8] Miller K, McArdle S, Gale M Jr, Geller DA, Tenoever B, Hiscott J, et al. Effects of the hepatitis C virus core protein on innate cellular defense pathways. J Interferon Cytokine Res 2004;24:391–402.

[9] Enomoto N, Sakuma I, Asahina Y, Kurosaki M, Murakami T, Yamamoto C, et al. Mutations in the nonstructural protein 5A gene and response to interferon in patients with chronic hepatitis C virus 1b infection. N Engl J Med 1996; 334:77–81.

[10] Kanda T, Yokosuka O, Imazeki F, Tanaka M, Shino Y, Shimada H, et al. Inhibition of subgenomic hepatitis C virus RNA in Huh-7 cells: ribavirin induces mutagenesis in HCV RNA. J Viral Hepat 2004;11:479–87.

[11] Akuta N, Suzuki F, Sezaki H, Suzuki Y, Hosaka T, Someya T, et al. Association of amino acid substitution pattern in core protein of hepatitis C virus genotype 1b high viral load and non-virological response to interferon-ribavirin combination therapy. Intervirology 2005;48:372–80.

[12] Donlin MJ, Cannon NA, Yao E, Li J, Wahed A, Taylor MW, et al. Pretreatment sequence diversity differences in the full-length hepatitis C virus open reading frame correlate with early response to therapy. J Virol 2007;81:8211–24.

[13] Akuta N, Suzuki F, Kawamura Y, Yatsuji H, Sezaki H, Suzuki Y, et al. Predictive factors of early and sustained responses to peginterferon plus ribavirin combination therapy in Japanese patients infected with hepatitis C virus genotype 1b: amino acid substitutions in the core region and low-density lipoprotein cholesterol levels. J Hepatol 2007;46: 403–10.

[14] Newton CR, Graham A, Heptinstall LE, Powell SJ, Summers C, Kalsheker N, et al. Analysis of any point mutation in DNA. The amplification refractory mutation system (ARMS). Nucleic Acids Res 1989;17:2503–16.

[15] Tada M, Omata M, Kawai S, Saisho H, Ohto M, Saiki R, et al. Detection of ras gene mutations in pancreatic juice and peripheral blood of patients with pancreatic adenocarcinoma. Cancer Res 1993;53:2472–4.

[16] Kanda T, Yokosuka O, Tagawa M, Kawai S, Imazeki F, Saisho H. Quantitative analysis of GBV-C RNA in liver and serum by strand-specific reverse transcription-polymerase chain reaction. J Hepatol 1998;29:707–14.

[17] Kanda T, Yokosuka O, Nagao K, Saisho H. State of hepatitis C viral replication enhances activation of NF-kB- and AP-1-signaling induced by hepatitis B virus X. Cancer Lett 2006;234:143–8.

[18] Okamoto K, Akuta N, Kumada H, Kobayashi M, Matsuo Y, Tazawa H. A nucleotide sequence variation detection system for the core region of hepatitis C virus-1b. J Virol Methods 2007;141:1–6.

[19] Kau A, Vermehren J, Sarrazin C. Treatment predictors of a sustained virologic response in hepatitis B and C. J Hepatol 2008;49:634–51.

[20] Herrmann E, Zeuzem S. Ribavirin plus either peginterferon alpha-2a or peginterferon alpha-2b for patients with chronic HCV infection? Nat Clin Pract Gastroenterol Hepat 2008;5: 362–3.

[21] Di Bisceglie AM, Ghalib RH, Hamzeh FM, Rustgi VK. Early virologic response after peginterferon alpha-2a plus ribavirin or peginterferon alpha-2b plus ribavirin treatment in patients with chronic hepatitis C. J Viral Hepat 2007;14: 721–9.

[22] Akuta N, Suzuki F, Kawamura Y, Yatsuji H, Sezaki H, Suzuki Y, et al. Amino acid substitutions in the hepatitis C virus core region are the important predictor of hepatocarcinogenesis. Hepatology 2007;46:1357–64.

[23] Kawai S, Yokosuka O, Kanda T, Imazeki F, Maru Y, Saisho H. Quantification of hepatitis C virus by TaqMan PCR: comparison with HCV Amplicor Monitor assay. J Med Virol 1999;58:121–6.

[24] Akuta N, Suzuki F, Hirakawa M, Kawamura Y, Yatsuji H, Sezaki H, et al. A matched case-controlled study of 48 and 72 weeks of peginterferon plus ribavirin combination therapy in patients infected with HCV genotype 1b in Japan: amino acid substitutions in HCV core region as predictor of sustained virological response. J Med Virol 2009;81:452–8.

[25] Lok AS, Seeff LB, Morgan TR, Di Bisceglie AM, Sterling RK, Curto TM, et al. Incidence of hepatocellular carcinoma and associated risk factors in hepatitis C-related advanced liver disease. Gastroenterology 2009;136:138–48.

Biochemical and Biophysical Research Communications 414 (2011) 331–336

Contents lists available at SciVerse ScienceDirect

Biochemical and Biophysical Research Communications

journal homepage: www.elsevier.com/locate/ybbrc

Senescence marker protein 30 (SMP30)/regucalcin (RGN) expression decreases with aging, acute liver injuries and tumors in zebrafish

Koichi Fujisawa [a], Shuji Terai [b,*], Yoshikazu Hirose [b], Taro Takami [c], Naoki Yamamoto [b], Isao Sakaida [a,b]

[a] Center for Reparative Medicine, Yamaguchi University School of Medicine, Minami Kogushi 1-1-1, Ube Yamaguchi 755-8505, Japan
[b] Department of Gastroenterology and Hepatology, Yamaguchi University Graduate School of Medicine, Minami Kogushi 1-1-1, Ube Yamaguchi 755-8505, Japan
[c] Division of Laboratory, Yamaguchi University Hospital, Minami-Kogushi 1-1-1, Ube Yamaguchi 755-8505, Japan

ARTICLE INFO

Article history:
Received 9 September 2011
Available online 17 September 2011

Keywords:
Zebrafish
Liver tumors
Aging
Senescence marker protein 30 (SMP30)
Regucalcin

ABSTRACT

Senescence marker protein 30 (SMP30)/regucalcin (RGN) is known to be related to aging, hepatocyte proliferation and tumorigenesis. However, expression and function of non-mammalian SMP30/RGN is poorly understood. We found that zebrafish SMP30/RGN mRNA expression decreases with aging, partial hepatectomy and thioacetamide-induced acute liver injury. SMP30/RGN expression was also greatly decreased in a zebrafish liver cell line. In addition, we induced liver tumors in adult zebrafish by administering diethylnitrosamine. Decreased expression was observed in foci, hepatocellular carcinomas, cholangiocellular carcinomas and mixed tumors as compared to the surrounding area. We thus showed the importance of SMP30/RGN in liver proliferation and tumorigenesis.

1. Introduction

Senescence marker protein 30 (SMP30) was originally identified by two-dimensional gel electrophoresis as a 34 KDa protein of which expression decreases by up to 40% in the aged rat liver without androgen dependence [1]. But it was subsequently found to be the same as regucalcin (RGN), a calcium-related protein without an EF-hand motif [2]. RGN has been intensively studied by Yamaguchi and Takahashi who reported that RGN regulates intracellular Ca^{2+} homeostasis by activating Ca^{2+} pump activity in the cell membrane [3]. Moreover, SMP30/RGN inhibits Ca^{2+}-dependent protein kinase, protein phosphatase and nitric oxidase synthase, and thereby inhibits cell proliferation [4]. SMP30/RGN is known to exist in a broad range of species from mammals to bacteria, and its expression in mammals is high in hepatic parenchymal cells and the renal cortex [5]. Compared with normal mice, SMP30/RGN knockout mice age more rapidly and have increased fat droplets and lysosomes in their livers. Furthermore, SMP30/RGN was shown to be gluconolactonase, an enzyme indispensable for vitamin C synthesis, and the relationship between vitamin C and aging appears to be important [6,7]. SMP30/RGN mRNA expression is reportedly decreased in chemically-induced tumors as compared to surrounding normal liver tissue, based on in situ hybridization [8]. Microarray analysis showed SMP30/RGN to be one of the down-regulated genes in the GST-P positive area [9]. Although overexpression of SMP30/RGN in hepatoma cells down-regulates oncogenes such as c-myc, Haras and c-src [10], details of how SMP30/RGN takes part in the development and progression of cancer remain unknown. Zebrafish are the simplest vertebrate model because of their low breeding costs and the capacity for high-through-put screening [11,12]. Zebrafish provide a good cancer model because various diethylnitrosamine (DEN)-induced tumors resemble human tumors [13]. There are no reports concerning zebrafish SMP30/RGN except a study on dioxin administration to embryos [14]. Moreover, the expression of SMP30/RGN in mixed tumors and cholangiocellular carcinomas has not previously been reported. In this study, we examined the importance of SMP30/RGN in aging, liver proliferation and liver tumorigenesis using the zebrafish model.

2. Materials and methods

2.1. Animals

Zebrafish were maintained in accordance with the Animal care Guidelines of Yamaguchi University. Fish were kept in tap water in plastic tanks and illuminated with fluorescent lighting set at 16 h light and 8 h dark.

2.2. Cell culture

An adult zebrafish liver cell line (ATCC CRL-2643) was cultured in ZFL medium as described by Ghosh et al. [15].

* Corresponding author. Fax: +81 836 222303.
E-mail address: terais@yamaguchi-u.ac.jp (S. Terai).

0006-291X/$ - see front matter © 2011 Elsevier Inc. All rights reserved.
doi:10.1016/j.bbrc.2011.09.067

2.3. DEN exposure

One-year old fish were exposed to 200 ppm DEN for 2 months. DEN solutions were changed every week to compensate for degradation. Following exposure, the fish were maintained in tap water without DEN for 4 months.

2.4. Quantitative RT-PCR

Total RNA was isolated with TRIzol (Invitrogen), and treated with Turbo DNase (Ambion). RT-PCR was performed by utilizing the step one plus real time PCR system and Fast SYBR Green Master Mix (Applied Biosystems). Specific primers for SMP30/RGN (5′-ACT ATG ACA TCC AAA CTG GAG GA-3′ and 5′-CTT CTG TGT CTA TGC ACA TAC CG-3′) were used. Elongation factor 1-alpha was used as an internal control.

2.5. Tissue collection and histology

Fish were killed and opened from the anal vent to the gills. The entire body was fixed with 4% paraformaldehyde in 0.1 M phosphate buffer (PB). The liver was dissected, dehydrated in alcohol and embedded in paraffin according to routine procedures. Serial sections were cut at a thickness of 3–5 μm. Staining was performed using hematoxylin and eosin (HE).

2.6. Immunohistochemistry (IHC)

Antibody for SMP30/RGN was obtained from Shima Laboratories (Tokyo, Japan). SMP30/RGN was immunohistochemically assessed using the avidin–biotin–peroxidase complex method, as described previously [16].

2.7. Western blot analysis

Samples were prepared by the same methods as previously reported [17]. The blots were incubated for 1 h at room temperature with primary antibodies against SMP30/RGN (Shima), and β-actin (Sigma) in blocking buffer. After being washed, the blots were incubated for 1 h at room temperature with secondary antibodies. Reactive bands were identified using an enhanced chemiluminescence kit (Amersham Biosciences) and autoradiography according to the manufacturer's instructions.

2.8. Partial hepatectomy

Liver regeneration was induced by partial hepatectomy. The ventral lobes of zebrafish livers were removed by the methods reported by Sadler et al. [18].

2.9. Thioacetamide (TAA) treatment

Six-month-old female zebrafish were injected with 300 mg/kg body TAA intraperitoneally. Two days after injection, the livers were collected and used for further examinations.

2.10. Statistical analysis

All data are expressed as means ± S.D. One way ANOVA followed by the Dunnett post hoc multiple comparison test was performed to assess the statistical significance of differences in SMP30/RGN expression with aging. The Kruskal–Wallis test followed by the Steel method was performed to assess the statistical significance of SMP30/RGN expression changes caused by partial hepatectomy. Student's *t*-test was performed to assess the results of other examinations. *P* values less than 0.05 were considered to be significant.

3. Results

3.1. Expression of SMP30/RGN in normal zebrafish tissues

SMP30/RGN is reportedly expressed in the livers and kidneys of mammals. We examined SMP30/RGN expression in various zebrafish tissues by Western blotting methods. The 35 KDa form was observed in livers, intestine and kidneys (Fig. 1A). We then examined immunohistochemical expression patterns and found that SMP30/RGN was expressed in hepatic parenchymal cells and the renal cortex of adult zebrafish (Fig. 1B).

3.2. SMP30/RGN expression changes with aging

Mammalian SMP30/RGN expression is known to decrease with aging. We examined SMP30/RGN expression changes in the liver with aging. We used 3-month-old, 6-month-old, 1-year-old and 3-year-old zebrafish. Body lengths were 19.6 ± 1.9, 22.9 ± 1.9, 28.7 ± 1.5, and 30.3 ± 3.2 mm (Fig. 2A), weights.7 ± 8.3, 295.8 ± 84.7, 493.0 ± 108.3, and 721.3 ± 259.3 mg (Fig. 2B), body mass index (BMI) 0.034 ± 0.002, 0.055 ± 0.009, 0.063 ± 0.008, and 0.076 ± 0.010 g/cm^2 (Fig. 2C), respectively. Three-year old zebrafish had spinal curvature which is a feature of advanced age (Fig. 2D). Fold changes in SMP30/RGN mRNA expression by quantitative RT-PCR were 1.00 ± 0.41,.0 0.43 ± 0.25, 0.41 ± 0.27, and 0.17 ± 0.05, respectively (Fig. 2E). SMP30/RGN expression thus decreased significantly with aging.

3.3. SMP30/RGN expression changes during regeneration after partial hepatectomy

We isolated total RNA from partially hepatectomized livers and regenerating livers after partial hepatectomy, and examined SMP30/RGN mRNA expressions by quantitative PCR with EF1a expression as an internal control. Expression of SMP30/RGN mRNA was significantly decreased to 50.0% ± 13.6% and 50.9% ± 10.4% 1

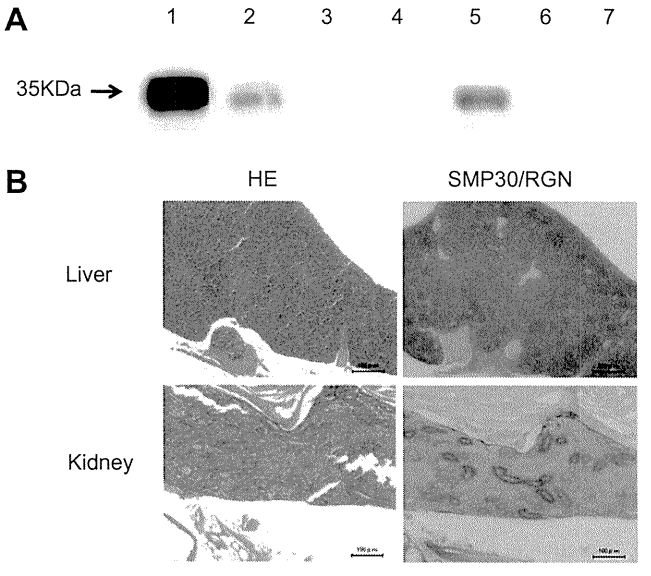

Fig. 1. SMP30/RGN expressions in various tissues in zebrafish. (A) SMP30/RGN expressions in various tissues. 1, liver; 2, intestine; 3, muscle; 4, brain; 5, kidney; 6, heart; 7, testicle. (B) IHC staining of zebrafish liver and kidney with polyclonal antibody for SMP30/RGN. Left: HE staining, right: anti-SMP30/RGN antibody, bar: 100 μm.

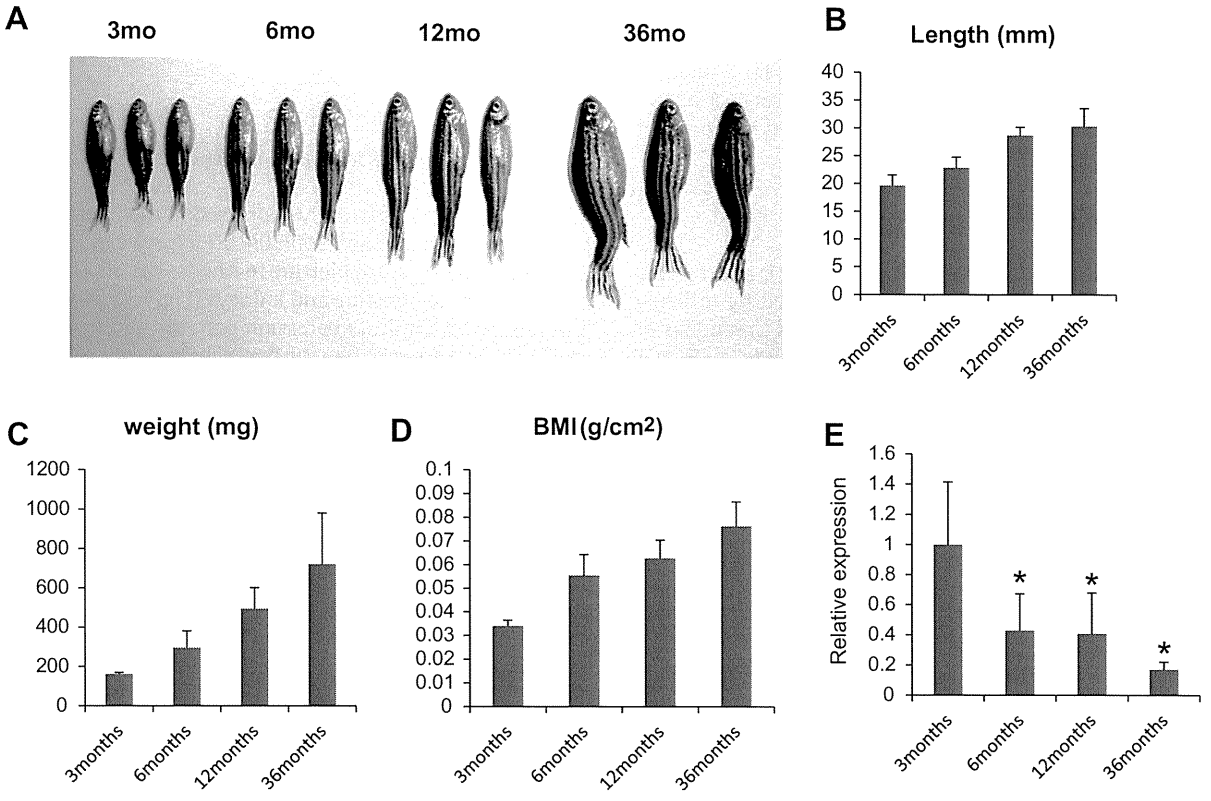

Fig. 2. Change of SMP30/RGN expression with aging. (A) Whole images of zebrafish at 3, 6, 12 and 36 months of age. (B) Body length (cm). (C) body weight (mg). (D) BMI (g/cm^2). Data are expressed as means ± S.D. (E) Expressions of SMP30/RGN mRNA changed with aging, EF1a is used as an internal control. Statistical analysis was performed by one-way ANOVA followed by Dunnett post hoc multiple comparison test, *indicates $P < 0.01$ between 3 months and the groups at 6, 12 and 36 months.

and 2 days after partial hepatectomy, respectively (Fig. 3A). No expression changes were observed 3 and 7 days after partial hepatectomy.

3.4. SMP30/RGN expression changes in acute liver injury induced by TAA administration

We examined expression of SMP30/RGN mRNA in the liver 48 h after intraperitoneal administration of TAA, a hepatotoxic agent, by quantitative RT-PCR. SMP30/RGN mRNA was significantly decreased in TAA-treated livers. Levels of SMP30/RGN expression in control and TAA livers were 1.00 ± 0.08 and 0.58 ± 0.09, respectively (Fig. 3B). The number of PCNA positive cells was increased in TAA-treated liver by IHC (Fig. 3C and D).

3.5. SMP30/RGN expression in zebrafish liver cell line

In order to examine expression of SMP30/RGN in proliferating cells, we used a zebrafish liver cell line (ZFL) (Fig. 4A). ZFL cells were derived from normal adult zebrafish liver, and synthesize and release several proteins into the culture medium, including a 70 kDa protein recognized by anti-bovine serum albumin IgG [15]. SMP30/RGN protein expression was significantly decreased, while PCNA expression was increased in ZFL cells as compared to normal liver extracts (Fig. 4B).

3.6. Induction of liver tumors by DEN administration

We maintained adult zebrafish with 200 ppm DEN solution for 2 months with weekly solution changes, and then kept them in tap water without DEN for 4 months to allow liver tumor development. We obtained some zebrafish with bulging abdomens (Fig. 4C). We then dissected these zebrafish and confirmed liver enlargement (Fig. 4D and D′).

3.7. SMP30/RGN expression in zebrafish liver tumors

We examined SMP30/RGN expressions in various liver tumors by IHC. Decreased SMP30/RGN expression and increased PCNA expression were observed in foci as compared to surrounding normal liver tissues (Fig. 4F and G). Decreased expression was observed in hepatocellular carcinomas (HCC) (Fig. 4I), which are characterized by complete loss of normal tubular architecture and compression of the peripheral area on HE staining (Fig. 4H). Increased PCNA-positive staining in the nuclear was also seen in HCC (Fig. 4J). We noted lower expressions in cholangiocellular carcinomas, which have highly developed ductal structures (Fig. 4K–M). We also recognized decreased SMP30/RGN expression in mixed cell tumors, which have irregular cords of small hepatocytes and small ductules of biliary epithelial cells (Fig. 4N–P). We checked all 18 DEN-treated zebrafish, and found three to have foci, six adenoma/HCC, three cholangiocellular carcinomas and four for mixed type tumors. We examined SMP30/RGN expression in each tumor by IHC, and found decreases in three of the four foci (75%), 15 of the 17 adenoma/HCC (88.2%), all three cholangiocellular carcinomas (100%) and all six mixed tumors (100%) (Table 1).

4. Discussion

SMP30 was originally reported to be a protein which is greatly reducing with aging [1]. Although the existence of SMP30/RGN was observed in various organisms, there are few reports concerning non-mammalian SMP30/RGN. Detailed SMP30 examination was reported for abalone, a marine invertebrate [19], but detailed

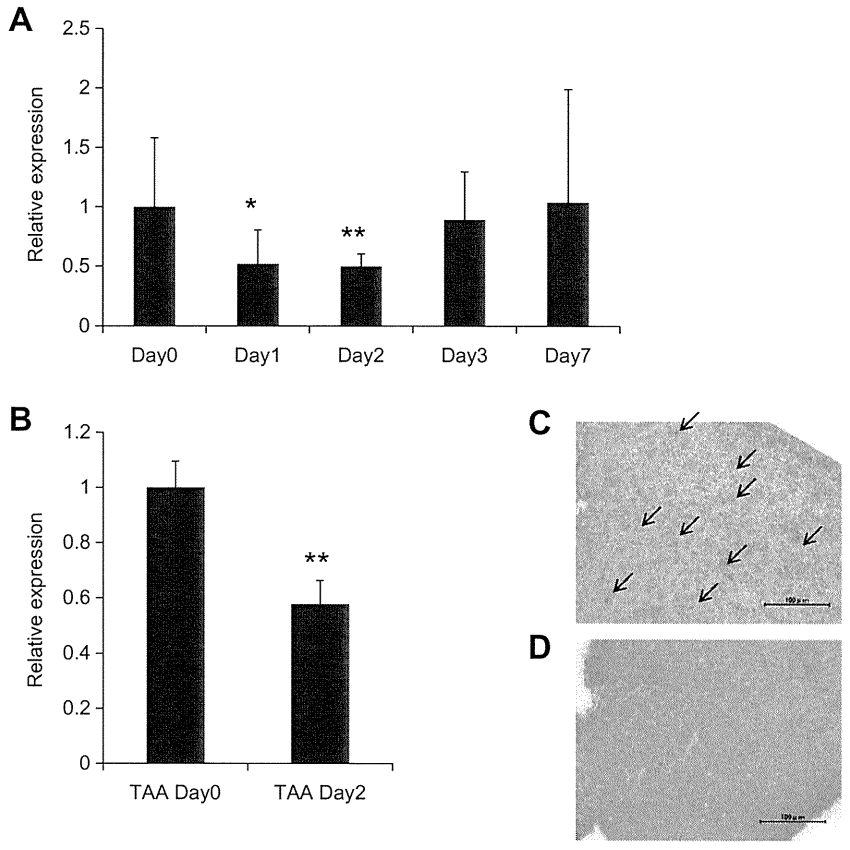

Fig. 3. SMP30/RGN mRNA expression in liver regeneration after partial hepatectomy and liver injury after TAA injection. (A) Expressions of SMP30/RGN mRNA after partial hepatectomy * and ** indicate $P < 0.05$ and 0.01 between control (Day 0) and partial hepatectomy group (Days 1–3 and 7). (B) SMP30/RGN mRNA expression changed in TAA-treated livers. (C) PCNA expression in TAA-treated liver, bar: 100 μm. Arrow indicated PCNA-positive cells. (D) PCNA expression incontrol liver. Bar: 100 μm.

examinations of zebrafish SMP30/RGN are lacking. We examined SMP30/RGN in zebrafish which is a good model for tumorigenesis and high-through-put screening is possible.

Zebrafish are becoming a new aging model [20]. Being different from mammals, teleosts keep growing in adulthood. In this study, 3-year-old zebrafish had 1.6 times the body length of a 6-month zebrafish. We examined whether SMP30/RGN mRNA expression decreases in the growing liver. We found SMP30/RGN mRNA expression to be significantly decreased with aging (Fig. 2E). SMP30/RGN has antioxidant properties that protect cells from oxidative stress, and overexpression of SMP30/RGN in a liver cell line contributed to a marked decrease in reactive oxygen species (ROS) formation as well as decreased lipid peroxidation, superoxide dismutase activity and glutathione levels [21]. Down-regulation of SMP30/RGN during the aging process may increase ROS formation. Moreover, calcium metabolism is important for understanding the aging process because it is related to electrolyte balance, calculus formation and osteoporosis. From the viewpoint of calcium metabolism, calbindin-D, a calcium binding protein, shows similar age-associated decreases in the brains of rats and humans. There is a possibility that the age-associated decrease in SMP30/RGN mRNA expression is related to calcium homeostasis, which deteriorates with aging.

SMP30/RGN mRNA expression is reportedly decreased 12 h after 70% partial hepatectomy, and then increased 2–3 days thereafter [22]. Zebrafish SMP30/RGN mRNA expression is decreased 1–2 days after partial hepatectomy. Overexpression of SMP30/RGN in hepatoma cells suppresses the expression of c-src but induces p53 and Rb expressions [23]. It is reasonable that SMP30/RGN expression is suppressed within 2 days after partial hepatectomy, when hepatocytic proliferation activity is high. However, in contrast to the mouse SMP30/RGN expression data, we found no increase in expression after partial hepatectomy. Partial hepatectomy is achieved in zebrafish by removing about 30% of the total liver, and the PCNA index peaks 48 h thereafter [18]. On the other hand, mouse partial hepatectomy requires that more than 70% of the liver be removed. There is a possibility that the zebrafish SMP30/RGN expression pattern differs from that in mice due to the smaller amount of liver removed. On the other hand, there was reportedly no increase in expression after partial hepatectomy in the mouse. A microarray analysis revealed that SMP30/RGN expression was decreased 12 h after partial hepatectomy, but there were no expression changes 1–2 days after partial hepatectomy [24]. The difference in expressions and the role of SMP30/RGN after partial hepatectomy require further investigation.

TAA is a centrilobular hepatotoxic agent which is metabolized by CYP2E1. Mice receiving a single dose of TAA are used as an acute liver injury model [25]. In this study, SMP30/RGN mRNA expression was decreased 48 h after TAA administration. TAA administration caused centrilobular necrosis and there was a subsequent regenerative response. As after partial hepatectomy, SMP30/RGN expression diminished when the liver was in a proliferative state.

Changes in SMP30/RGN expression in some tumor types such as breast cancer, prostate cancer and HCC were reported [26]. At the transcriptional level, SMP30/RGN mRNA was profiled as being a down-regulated gene in rat GST-P positive DEN-induced lesions as compared to the surrounding area [9]. A clinical proteomic study showed SMP30/RGN expression to be decreased in tumors [27].

In this study, we found expression of SMP30/RGN protein to be decreased in a zebrafish liver cell line (Fig. 4B) and in DEN-induced

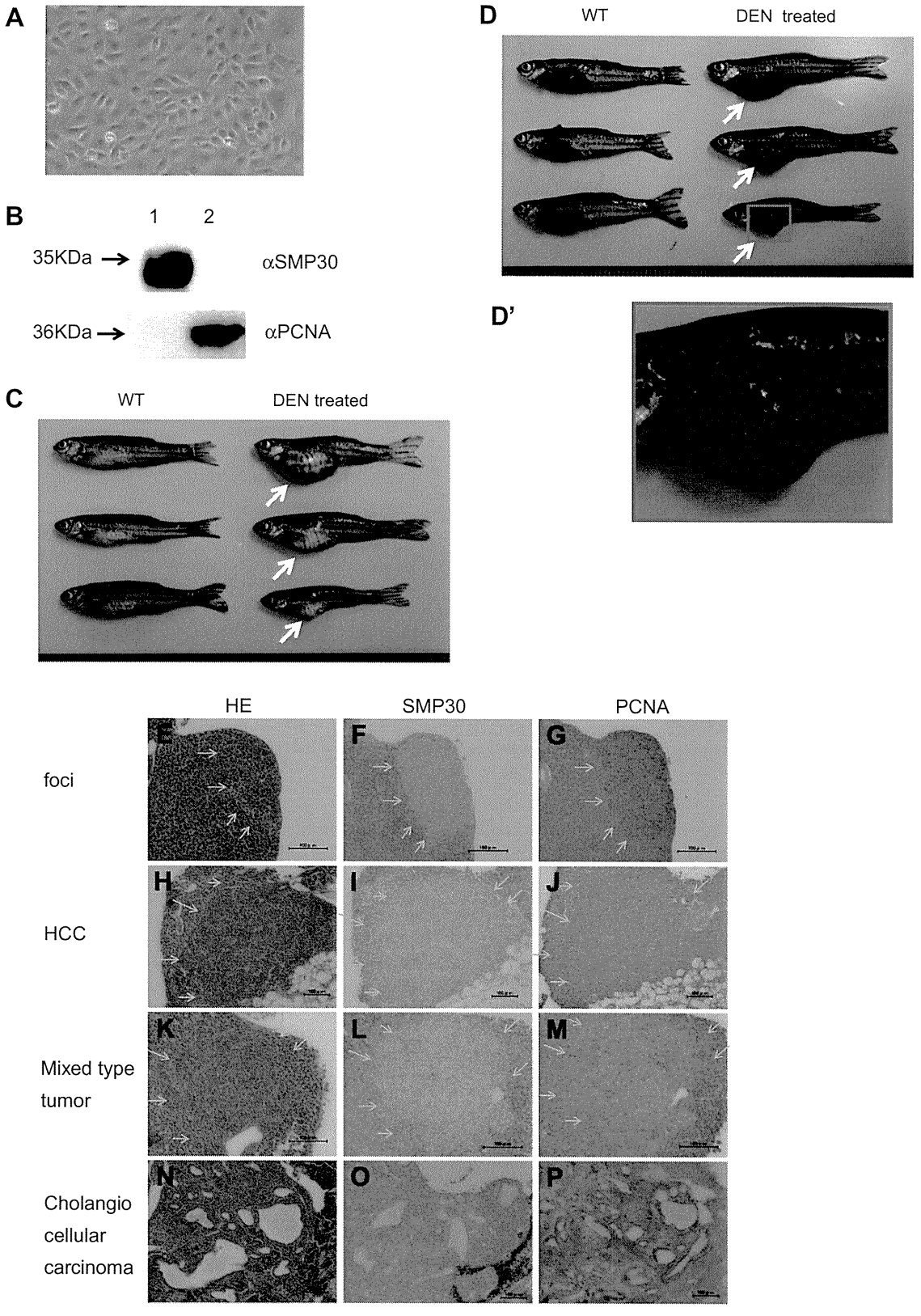

Fig. 4. SMP30/RGN expression in zebrafish liver tumor. (A) Photomicrograph of ZFL. (B) Expressions of SMP30/RGN and PCNA in normal liver and zebrafish liver cell line. (C) Whole image of DEN-treated zebrafish: arrows indicate bulging abdomen. (D) Image from DEN-treated zebrafish: arrows indicate liver tumor. (D′) High-power field of swollen liver. (E–P) IHC analyses of various liver tumors. Left: HE staining, middle: anti-SMP30/RGN antibody, right: anti-PCNA antibody, bar: 100 μm. (E–G) foci, (H–J) HCC, (K–M) mixed type tumor, (N–P) cholangiocellular carcinoma. Arrows indicate boundary of tumor and surrounding area.

foci and adenoma/HCC, as compared to surrounding tissues (Fig. 4E–J). Furthermore, SMP30/RGN expression was decreased in mixed tumors and cholangiocellular carcinomas. This is, to our knowledge, the first report of SMP30/RGN expressions in these

Table 1
Expression of SMP30/RGN in zebrafish tumors induced by DEN treatment.

	Number of fish with tumors/ total number of fish examined	Total number of tumors	Number of tumors with decreased SMP30 expression	Ratio of SMP30 decreased tumors (%)
Foci	3/18	4	3	75
Adenoma/HCC	6/18	17	15	88
Mixed tumor	4/18	6	6	100
Cholangiocellular carcinoma	3/18	3	3	100

two tumors. Mixed tumors are a rare type of primary hepatic tumor thought to originate from a single site, but with two possible endpoints of differentiation. Cholangiocellular carcinoma is an adenocarcinoma and the actual cell origin is unknown, although it has been suggested to arise from pluripotent hepatic stem cells. Overexpression of SMP30/RGN in HepG2 suppresses cell proliferation and expressions of oncogenes, while increasing the expressions of tumor suppressor genes [28]. In addition, the frequency of antibody against SMP30/RGN is significantly higher in well-differentiated than in poorly-differentiated HCC [26]. We thus speculate that reduced SMP30/RGN expression enhances cell proliferation and is ultimately related to tumor progression. SMP30/RGN expression reduction was observed at a high frequency in tumors (Table 1). SMP30/RGN would thus be a good marker for liver various tumors.

In conclusion, we demonstrated the importance of SMP30/RGN in aging, partial hepatectomy, acute liver injury and liver tumorigenesis. SMP30/RGN has multiple functions in aging, proliferation and tumorigenesis, but physiological roles of SMP30/RGN have yet to be fully elucidated. Detailed investigations of the functions of SMP30/RGN are needed.

Acknowledgments

We thank Dr. M. Furutani-Seiki for technical advices and Ms. M. Yamada, Ms. I. Fujimoto and Ms. Y. Fukusumi for their technical assistance. This study was supported by Grants-in-Aid for Scientific Research (22390150) and a Grant-in-Aid for Challenging Exploratory Research (22659148, 23659398) from the Japan Society for the Promotion of Science.

References

[1] T. Fujita, K. Uchida, N. Maruyama, Purification of senescence marker protein-30 (SMP30) and its androgen-independent decrease with age in the rat liver, Biochim. Biophys. Acta 1116 (1992) 122–128.
[2] N. Shimokawa, M. Yamaguchi, Molecular cloning and sequencing of the cDNA coding for a calcium-binding protein regucalcin from rat liver, FEBS Lett. 327 (1993) 251–255.
[3] H. Takahashi, M. Yamaguchi, Role of regucalcin as an activator of Ca(2+)-ATPase activity in rat liver microsomes, J. Cell. Biochem. 74 (1999) 663–669.
[4] T. Ishigami, T. Fujita, G. Simbula, A. Columbano, K. Kikuchi, A. Ishigami, T. Shimosawa, Y. Arakawa, N. Maruyama, Regulatory effects of senescence marker protein 30 on the proliferation of hepatocytes, Pathol. Int. 51 (2001) 491–497.
[5] M. Yamaguchi, M. Isogai, Tissue concentration of calcium-binding protein regucalcin in rats by enzyme-linked immunoadsorbent assay, Mol. Cell. Biochem. 122 (1993) 65–68.
[6] A. Ishigami, Y. Kondo, R. Nanba, T. Ohsawa, S. Handa, S. Kubo, M. Akita, N. Maruyama, SMP30 deficiency in mice causes an accumulation of neutral lipids and phospholipids in the liver and shortens the life span, Biochem. Biophys. Res. Commun. 315 (2004) 575–580.
[7] Y. Kondo, Y. Inai, Y. Sato, S. Handa, S. Kubo, K. Shimokado, S. Goto, M. Nishikimi, N. Maruyama, A. Ishigami, Senescence marker protein 30 functions as gluconolactonase in L-ascorbic acid biosynthesis, and its knockout mice are prone to scurvy, Proc. Natl. Acad. Sci. USA 103 (2006) 5723–5728.
[8] R. Makino, M. Yamaguchi, Expression of calcium-binding protein regucalcin mRNA in hepatoma cells, Mol. Cell. Biochem. 155 (1996) 85–90.
[9] S. Suzuki, M. Asamoto, K. Tsujimura, T. Shirai, Specific differences in gene expression profile revealed by cDNA microarray analysis of glutathione S-transferase placental form (GST-P) immunohistochemically positive rat liver foci and surrounding tissue, Carcinogenesis 25 (2004) 439–443.
[10] M. Yamaguchi, Y. Daimon, Overexpression of regucalcin suppresses cell proliferation in cloned rat hepatoma H4-II-E cells: involvement of intracellular signaling factors and cell cycle-related genes, J. Cell. Biochem. 95 (2005) 1169–1177.
[11] T. Matsumoto, S. Terai, T. Oishi, S. Kuwashiro, K. Fujisawa, N. Yamamoto, Y. Fujita, Y. Hamamoto, M. Furutani-Seiki, H. Nishina, I. Sakaida, Medaka as a model for human nonalcoholic steatohepatitis, Dis. Model. Mech. 3 (2010) 431–440.
[12] S. Terai, Fish model leads to new findings in liver disease, Hepatol. Res. 40 (2010) 111–113.
[13] W. Goessling, T.E. North, L.I. Zon, New waves of discovery: modeling cancer in zebrafish, J. Clin. Oncol. 25 (2007) 2473–2479.
[14] Y.D. Wu, L. Jiang, Z. Zhou, M.H. Zheng, J. Zhang, Y. Liang, CYP1A/regucalcin gene expression and edema formation in zebrafish embryos exposed to 2,3,7,8-tetrachlorodibenzo-p-dioxin, Bull. Environ. Contam. Toxicol. 80 (2008) 482–486.
[15] C. Ghosh, Y.L. Zhou, P. Collodi, Derivation and characterization of a zebrafish liver cell line, Cell Biol. Toxicol. 10 (1994) 167–176.
[16] S. Kuwashiro, S. Terai, T. Oishi, K. Fujisawa, T. Matsumoto, H. Nishina, I. Sakaida, Telmisartan improves nonalcoholic steatohepatitis in medaka (*Oryzias latipes*) by reducing macrophage infiltration and fat accumulation, Cell Tissue Res. 344 (2011) 125–134.
[17] K. Fujisawa, R. Murakami, T. Horiguchi, T. Noma, Adenylate kinase isozyme 2 is essential for growth and development of *Drosophila melanogaster*, Comp. Biochem. Physiol. B Biochem. Mol. Biol. 153 (2009) 29–38.
[18] K.C. Sadler, K.N. Krahn, N.A. Gaur, C. Ukomadu, Liver growth in the embryo and during liver regeneration in zebrafish requires the cell cycle regulator, uhrf1, Proc. Natl. Acad. Sci. USA 104 (2007) 1570–1575.
[19] C. Nikapitiya, M. De Zoysa, H.S. Kang, C. Oh, I. Whang, J. Lee, Molecular characterization and expression analysis of regucalcin in disk abalone (*Haliotis discus* discus): intramuscular calcium administration stimulates the regucalcin mRNA expression, Comp. Biochem. Physiol. B Biochem. Mol. Biol. 150 (2008) 117–124.
[20] S. Kishi, B.E. Slack, J. Uchiyama, I.V. Zhdanova, Zebrafish as a genetic model in biological and behavioral gerontology: where development meets aging in vertebrates – a mini-review, Gerontology 55 (2009) 430–441.
[21] S. Handa, N. Maruyama, A. Ishigami, Over-expression of Senescence Marker Protein-30 decreases reactive oxygen species in human hepatic carcinoma Hep G2 cells, Biol. Pharm. Bull. 32 (2009) 1645–1648.
[22] T. Katsumata, M. Yamaguchi, Inhibitory effect of calcium-binding protein regucalcin on protein kinase activity in the nuclei of regenerating rat liver, J. Cell. Biochem. 71 (1998) 569–576.
[23] T. Izumi, M. Yamaguchi, Overexpression of regucalcin suppresses cell death in cloned rat hepatoma H4-II-E cells induced by tumor necrosis factor-alpha or thapsigargin, J. Cell. Biochem. 92 (2004) 296–306.
[24] M. Arai, O. Yokosuka, T. Chiba, F. Imazeki, M. Kato, J. Hashida, Y. Ueda, S. Sugano, K. Hashimoto, H. Saisho, M. Takiguchi, N. Seki, Gene expression profiling reveals the mechanism and pathophysiology of mouse liver regeneration, J. Biol. Chem. 278 (2003) 29813–29818.
[25] T.M. Chen, Y.M. Subeq, R.P. Lee, T.W. Chiou, B.G. Hsu, Single dose intravenous thioacetamide administration as a model of acute liver damage in rats, Int. J. Exp. Pathol. 89 (2008) 223–231.
[26] C. Maia, C. Santos, F. Schmitt, S. Socorro, Regucalcin is under-expressed in human breast and prostate cancers: effect of sex steroid hormones, J. Cell. Biochem. 107 (2009) 667–676.
[27] W. Kim, S. Oe Lim, J.S. Kim, Y.H. Ryu, J.Y. Byeon, H.J. Kim, Y.I. Kim, J.S. Heo, Y.M. Park, G. Jung, Comparison of proteome between hepatitis B virus- and hepatitis C virus-associated hepatocellular carcinoma, Clin. Cancer Res. 9 (2003) 5493–5500.
[28] Y. Tsurusaki, M. Yamaguchi, Overexpression of regucalcin modulates tumor-related gene expression in cloned rat hepatoma H4-II-E cells, J. Cell. Biochem. 90 (2003) 619–626.

肝癌幹細胞を探る

寺井崇二* 坂井田功*

KEY WORDS

肝癌幹細胞，肝前駆細胞，肝細胞癌

SUMMARY

肝細胞癌は肝硬変の進展に伴い発癌率が増加する．つまりは線維化進行というニッチは，発癌が誘導されやすい環境であり，肝細胞癌は多中心性に発癌する．近年の fluorescence activated cell sorting（FACS）技術の進歩による肝臓構成細胞の分離技術の進歩，また人工多能性幹細胞（induced pluripotent stem cell：iPS 細胞）の発見より“成熟した細胞も簡単に初期化する”ことが明らかになり，従来とは違う研究アプローチ，視点から，肝細胞癌のなかの抗癌剤耐性の癌幹細胞（cancer stem cell）の研究が進められ，新たに“肝癌幹細胞”の報告があいついできた．また肝癌幹細胞の制御機構についても，メチル化，マイクロ RNA（miRNA）による制御，transforming growth factor（TGF）-β など各種サイトカインとの関連などさまざまな報告がされてきた．本稿においては，最近の肝癌幹細胞の研究について紹介し，従来の肝発癌の考えと比較し，その重要について概説する．

はじめに

肝細胞癌の発生率は，日本国内では全癌のなかで第4位である．肝線維化の進行，すなわち慢性肝炎から肝硬変症の進行とともに，肝発癌率が増加する．肝障害の進行に伴い，肝線維化が進行し，その結果多中心性の発癌を示す．肝硬変進行のなかでの肝前駆細胞の発生，増殖の理解が重要である．肝臓領域において最近になり急速に肝幹細胞，肝癌幹細胞の研究成果が集積している．この一因としては，モノクローナル抗体および fluorescence activated cell sorting（FACS）技術にて，肝臓構成細胞を細胞膜抗原の発現により厳密に識別・分離して性状を解析することできるようになってきたことによる．肝癌幹細胞の発見は，癌自体はヘテロな細胞集団であり，そのなかに抗癌剤耐性の癌幹細胞（cancer stem cell）があることが明らかになりつつあり，癌の制御の問題を考えるうえで重要である．一方で，従来の肝発癌の考え方との協調的な理解は十分でない．この理由としては，従来の肝発癌の理解では，dysplastic nodule などの前癌性病変を経て肝細胞癌ができるという考えであった

* Terai Shuji, Sakaida Isao/山口大学大学院医学系研究科消化器病態内科学

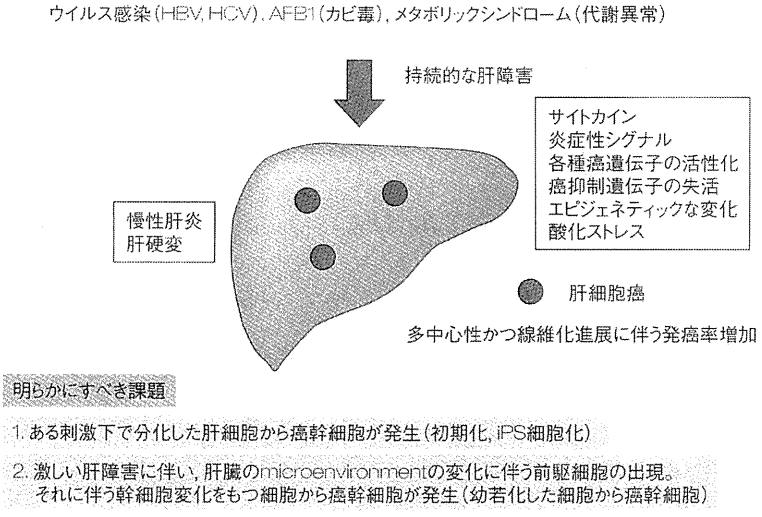

図❶　肝細胞癌の特徴と癌幹細胞の意味

が，人工多能性幹細胞（induced pluripotent stem cell：iPS細胞）の発見などより，成熟した細胞も特殊な刺激下では簡単に初期化することが明らかになったことより，成熟肝細胞から癌幹細胞が発生する可能性は十二分に推察されることになった．図❶では簡単に，今の肝癌の知見，および本稿でより明らかにしたい点を提示する．それにより肝癌幹細胞の新たな知見を理解してもらい，今後の肝癌幹細胞研究の重要性について論じたい．

肝幹細胞，前駆細胞と肝癌幹細胞

"幹細胞"の定義としては，"自己複製能と分化能をもった細胞"で，一番明確なのが造血幹細胞である．骨髄中の造血幹細胞は生涯にわたり維持され，大量の血球をつくりつづける．細胞表面マーカーを使って純化した造血幹細胞を一個移植すれば，それに由来する血球が何ヵ月もつくられるので，造血幹細胞についてはきわめて厳密に定義される．肝幹細胞は幹細胞の厳密な定義にはあてはまらないものの，"クローン増殖ができて，しかも胆管と肝細胞への分化能をもった細胞"が"肝幹細胞"と考えられている．一方，前駆細胞の増殖は一過性であり，長期に増殖しない細胞である．発生過程で出現する肝芽細胞は，増殖能と2方向への分化能をもった肝幹細胞とみなされる[1)2)]．また，成体肝臓の重篤な肝障害に伴い，肝細胞，胆管細胞の両方の性質をもった細胞が門脈周辺に発生するが，この細胞の核が卵円形のであることから，Oval細胞ともよばれている．Oval細胞は胆管細胞，肝細胞に分化することから（図❷），従来，肝幹細胞とみなされていた．しかし，最近の研究では，大部分のOval細胞は一過性に増殖する前駆細胞であると考えられている．Oval細胞の起源は胆管と肝細胞索のあいだのヘリング管との説が有力であったが，細胞系譜解析から肝細胞からも発生するとの報告もあり，その起源については議論があり明らかでない．図❸は，肝幹細胞，肝前駆細胞の制御機構についての最近の知見をまとめたものであるが，マクロファージ，肝星細胞などから構成されるさまざまな分化ニッチの制御により，肝幹細胞は制御される．またこのような前駆細胞の発生をつうじてまた逆に周囲の環境を制御し，その結果組織修復が進むと考えられる[3)]．

癌幹細胞の概念そのものは150年前の"embryonal rest hypothesis"を基盤としており，"癌細胞は胎児期の細胞と同じ表現型"をとることから提唱された．多くの癌組織は階層性をもった不均一な細胞集団であり，癌組織中の一部の細胞のみが増殖能と分化能をもち，それらは免疫不全マウスに移植すると癌をつくることができることから，"tumor initiating cell"ともよばれている．こうした癌幹細胞の存在は，白血病[4)]，脳腫瘍[4)]，乳癌[5)]をは